Spatial Modulation and Topological Current in Holographic QCD Matter

Kenji Fukushima and Pablo A. Morales
Department of Physics, Keio University, Kanagawa 223-8522, Japan
(Received 29 May 2013; published 31 July 2013)

We investigate an impact of the axial-vector interaction on the spatial modulation of quark matter. A magnetic field coupled with baryon density leads to a topological axial current so that the effect of the axial-vector interaction is then crucially enhanced. Using the Sakai-Sugimoto model, we have found that contrary to a naive expectation, the spatially modulated phase is less favored for a stronger magnetic field, which is realized by the presence of topological current.

DOI: 10.1103/PhysRevLett.111.051601 PACS numbers: 11.25.Tq, 12.38.Mh, 12.38.−t

Introduction.—The phase diagram of hot and dense matter out of quarks and gluons has not been clarified satisfactorily based on the first-principles theory of the strong interaction, i.e., quantum chromodynamics (QCD). The most severe obstacle is the notorious sign problem of the Dirac determinant at finite quark density ρ or chemical potential μ, which prevents us from the direct application of the Monte Carlo simulation in the region with $\mu \gtrsim T$ [1].

Instead of the lattice simulation, one could have deduced possible phase structures using chiral effective models, see, e.g., Ref. [2] for a recent work. It is conjectured from model studies that the chiral phase transition might be of first order at high density, so that a second-order critical point called the QCD critical point [3] could appear on the phase diagram, the discovery of which is one of the major goals of the beam-energy scan program in heavy-ion collision experiments [4]. The model setup, however, suffers from uncontrolled uncertainties and the QCD critical point is a model-dependent prediction. It is well understood by now that the vector-type interaction $\sim(\bar{\psi}\gamma_\mu\psi)^2$, which gives rise to the density-density interaction $\sim\rho^2$ even in the mean-field level, crucially affects the liquid-gas phase transition of dense quark matter [5,6] (see also Ref. [7]). Moreover, nowadays, spatially inhomogeneous states are becoming a more and more realistic candidate that may supersede the conventional first-order phase boundary [8], which is rather robust against the vector interaction [6,9].

The simplest ansatz to introduce spatial modulation is the chiral spiral or the dual chiral-density wave,

$$\langle\bar{\psi}\psi\rangle = \Delta\cos(\boldsymbol{k}\cdot\boldsymbol{x}), \quad \langle\bar{\psi}\gamma_5\tau^3\psi\rangle = \Delta\sin(\boldsymbol{k}\cdot\boldsymbol{x}), \qquad (1)$$

which is reminiscent of the p-wave π^0 condensate in symmetric nuclear matter. Recalling the history of the pion condensation [10], one may well consider that a spin-isospin short-range interaction could significantly diminish the reality of chiral spirals; it is indeed the case for the pion condensation that is disfavored by the so-called Landau-Migdal parameters g' associated with short-range effective interaction in Fermi liquid theory (see also Ref. [11] for some arguments in favor of the pion condensation). Thus, in the relativistic language, it is conceivable that the axial-vector interaction $\sim(\bar{\psi}\gamma_5\gamma_\mu\boldsymbol{\tau}\psi)^2$ may be influential on spatial modulation of quark matter, though the vector interaction is not. This is an important question but, to the best of our knowledge, there is no theoretical investigation on this issue. The difficulty lies in the fact that the axial vector has no mean-field contribution unlike the density in the vector channel, and therefore one should go beyond the mean-field approximation. So far, the renormalization-group improvement has been successful for the homogeneous states only [2].

This situation would be drastically changed if we turn on an external magnetic field B. Such a system of dense quark matter at strong magnetic field has been intensely investigated. It was pointed out first in the Sakai-Sugimoto model [12], which is a holographic dual of large-N_c QCD, that B lowers the critical μ [13]. This observation turns out to be generic in chiral models [14] and is often referred to as the inverse magnetic catalysis in contrast to the enhancement of chiral-symmetry breaking at zero density [15]. In this way, clarification of the QCD phase diagram along the larger-B direction is an intriguing subject and many studies have been devoted to it [16].

There are also some theoretical works focused on inhomogeneous states of dense quark matter at finite B: in the strong-B limit, quarks are dimensionally reduced into a $(1+1)$-dimensional system, so that the ground-state structure should be a chiral spiral, i.e., chiral magnetic spiral [17]. It is also possible that another spiral can develop due to the presence of B [18]. In view of such results, it should be a natural expectation that a stronger B may ease a barrier to form spirals.

Here, in this Letter, we address one important physical effect that has been overlooked in these preceding works. That is, the inevitable generation of the topological current,

$$\boldsymbol{j}_A = N_c\sum_f \frac{q_f^2\mu}{2\pi^2}\boldsymbol{B}, \qquad (2)$$

having the origin in quantum anomaly [19], should be incorporated. N_c is the number of colors, f runs over flavor degrees of freedom, and q_f is the electric charge of flavor f. Interestingly, if $\boldsymbol{j}_A \neq 0$ at finite μ and B, the axial-vector interaction has a mean-field contribution $\boldsymbol{j}_A^2$ in the same way as ρ^2 emerging from the vector interaction, which could have played a role similar to the Landau-Migdal interaction and thus disfavored spirals contrary to the naive expectation. Although there are numerous works that study such chiral magnetic and separation effects as in Eq. (2), nobody has ever considered its impact on the phase structure at finite μ and B.

For the purpose of addressing these issues, the Sakai-Sugimoto model suits us best. We could use conventional methods, but then it is difficult to quantify the axial-vector interaction. There is no such ambiguity in the holographic approach. Besides, the holographic technique for the phase diagram research has been successfully advanced recently, and the instability toward the spatially modulated phase has been discovered [20]. In the presence of chiral chemical potential, also, similar instability leading to a spiral has been identified in the Sakai-Sugimoto model [21].

Holographic description.—The gauge-gravity (or generally bulk-boundary) correspondence states that the full quantum generating functional of four-dimensional field theory is equivalent to the on-shell action of the gravity theory with corresponding source at the ultraviolet (UV) boundary. Thus, N_c $D4$ branes compactified along the x_4 direction represent the gluonic degrees of freedom [22], and N_f $D8$-$\overline{D8}$ branes realize the spontaneous breaking of $\mathrm{U}(N_f)_\mathrm{L} \times \mathrm{U}(N_f)_\mathrm{R}$ chiral symmetry in QCD [12]. In the same way as in the first paper of Ref. [20], we focus on the situation where $D8$ and $\overline{D8}$ are separate above the deconfinement transition. There, the induced metric on the flavor branes is

$$ds^2 = u^{3/2}[f(u)d\tau^2 + d\boldsymbol{x}^2] + \left[u^{3/2}x_4'(u)^2 + \frac{1}{u^{3/2}f(u)}\right]du^2, \qquad (3)$$

where $f(u) = 1 - u_T^3/u^3$. We note that all variables are made dimensionless by the anti–de Sitter (AdS) radius. The horizon at $u = u_T$ defines the Hawking temperature, which is translated to the physical temperature as $T = 3u_T^{1/2}/(4\pi)$. In the chiral symmetric phase, $D8$ and $\overline{D8}$ are simply straight so that $x_4'(u) = 0$ is chosen.

Then, the Dirac-Born-Infeld (DBI) action in the flavor sector can be expressed with the metric from Eq. (3) and the U(1) field strength tensor $F_{\alpha\beta}$ which is split into B in the z direction (under the simplification that all N_f flavors have the same electric charge), the background $\bar{a}_0$ and $\bar{a}_z$ corresponding to μ and j_A^z, and spatially inhomogeneous fluctuations $f_{\alpha\beta}$. The five-dimensional effective action reads

$$S_{D8}^{\mathrm{DBI}} = \mathcal{N}\int d\tau d^3x du u^{1/4}\sqrt{-\det(g_{\alpha\beta} + F_{\alpha\beta})} = \mathcal{N}\int d\tau d^3x du u^{5/2}\sqrt{\mathcal{A}\cdot\mathcal{B}}(1 + \mathcal{X}), \qquad (4)$$

with an overall (irrelevant) constant $\mathcal{N}$ and

$$\mathcal{A} = 1 - \bar{a}_0'(u)^2 + f(u)\bar{a}_z'(u)^2, \qquad \mathcal{B} = 1 + B^2u^{-3}, \quad (5)$$

and the fluctuation part $\mathcal{X}$ up to the quadratic order with respect to $f_{xy} = \partial_x a_y - \partial_y a_x$, and f_{yz}, f_{zx}, f_{ux}, f_{uy}, f_{uz} with similar definitions.

Hence, together with the Chern-Simons (CS) action, $S^{\mathrm{CS}} = (\mathcal{N}/8)\int d\tau d^3x du \epsilon^{\mu_1\mu_2\mu_3\mu_4\mu_5}A_{\mu_1}F_{\mu_2\mu_3}F_{\mu_4\mu_5}$, we can define variables conjugate to $\bar{a}_0'$ and $\bar{a}_z'$ using the full action $S = S_{D8}^{\mathrm{DBI}} + S^{\mathrm{CS}}$ as

$$\rho = -\frac{\delta S}{\delta \bar{a}_0'(u)} = u^{5/2}\bar{a}_0'(u)\sqrt{\frac{\mathcal{B}}{\mathcal{A}}} - 3B\bar{a}_z(u), \qquad (6)$$

$$b = \frac{\delta S}{\delta \bar{a}_z'(u)} = u^{5/2}f(u)\bar{a}_z'(u)\sqrt{\frac{\mathcal{B}}{\mathcal{A}}} - 3B\bar{a}_0(u). \qquad (7)$$

Because S is not dependent on $\bar{a}_0$ and $\bar{a}_z$ but on $\bar{a}_0'$ and $\bar{a}_z'$ only, ρ and b fixed from the equations of motion are u independent. We find $b = 0$ by evaluating it at $u = u_T$, and from the boundary condition $\bar{a}_0(\infty) = \mu$, we can get the asymptotic forms as

$$\bar{a}_z(u) \simeq -2\mu B u^{-3/2}, \qquad \bar{a}_0(u) \simeq \mu - \tfrac{9}{8}\rho u^{-3/2} \qquad (8)$$

near the UV boundary ($u \sim \infty$). This asymptotic behavior of $\bar{a}_z(u)$ represents the topological vector and axial-vector currents (2) [13,14,21,23]. In our numerical calculations, we fully solve Eqs. (6) and (7) for a given density ρ to obtain the whole profile of $\bar{a}_0(u)$ and $\bar{a}_z(u)$.

From the concrete form of $\mathcal{X}$ we can get the equations of motion with respect to fluctuations a_i ($i = x, y, z$) as

$$u^{-1/2}\sqrt{\frac{\mathcal{A}}{\mathcal{B}}}\left(\frac{\partial_y f_{yx}}{\mathcal{B}} + \mathcal{C}\partial_z f_{zx}\right) + \partial_u\left[\frac{u^{5/2}f(u)f_{ux}}{\sqrt{\mathcal{A}\cdot\mathcal{B}}}\right] + 3\bar{a}_0' f_{yz} = 0, \qquad (9)$$

$$u^{-1/2}\sqrt{\frac{\mathcal{A}}{\mathcal{B}}}\left(\frac{\partial_x f_{xy}}{\mathcal{B}} + \mathcal{C}\partial_z f_{zy}\right) + \partial_u\left[\frac{u^{5/2}f(u)f_{uy}}{\sqrt{\mathcal{A}\cdot\mathcal{B}}}\right] + 3\bar{a}_0' f_{zx} = 0, \qquad (10)$$

$$u^{-1/2}\sqrt{\frac{\mathcal{A}}{\mathcal{B}}}\mathcal{C}(\partial_x f_{xz} + \partial_y f_{yz}) + \partial_u\left[u^{5/2}\sqrt{\frac{\mathcal{B}}{\mathcal{A}}}\mathcal{C}f(u)f_{uz}\right] + 3\bar{a}_0' f_{xy} = 0, \qquad (11)$$

where $\mathcal{C} = 1 - f(u)\bar{a}_z'(u)^2/\mathcal{A}$.

Numerical results.—A finite B breaks rotational symmetry, and we cannot find the eigenmodes as done in Ref. [20]. Let us here explain how to proceed to the numerical analyses. Our goal is to locate the critical ρ or μ (denoted by μ_c hereafter) at which Eqs. (9)–(11) have normalizable solutions with some momenta k_x, k_y, k_z in Fourier space. In fact, the normalizability condition or the boundary conditions $a_i(\infty) \to 0$ dictate how the energy dispersion relations behave. Since we drop the time dependence, our solutions describe the dispersion relation at zero energy. If a zero-energy excitation is realized with nonzero momenta, a homogeneous state should become unstable.

To solve three differential equations for a_i from $u = u_T$ to $u = \infty$, we need to specify the initial condition for $a_i'(u_T)$. These are uniquely taken if we require the solutions to be nonsingular at $u = u_T$; since $f(u)$ vanishes at $u = u_T$, only the term with ∂_u acting on $f(u)$ remains nonzero unless $a_i''(u_T)$ is singular. Then, we can easily express $a_i'(u_T)$ using $a_i(u_T)$. For example, we can deduce $a_x'(u_T)$ from Eq. (9) as

$$a_x'(u_T) = \frac{\mathcal{A}}{3u_T^2}\left[\frac{k_y^2 a_x - k_x k_y a_y}{\mathcal{B}} + \mathcal{C}(k_z^2 a_x - k_z k_x a_z)\right] - i\sqrt{\mathcal{A}\cdot\mathcal{B}}\,\bar{a}_0' u_T^{-3/2}(k_y a_z - k_z a_y), \qquad (12)$$

as well as $a_y'(u_T)$ and $a_z'(u_T)$ similarly.

Now, we are ready to solve Eqs. (9)–(11) numerically, and the final values $a_i(\infty)$ are then given as functions of the initial values $a_i(u_T)$, which can be expressed, thanks to the linearity, as follows:

$$\begin{pmatrix} a_x(\infty) \\ a_y(\infty) \\ a_z(\infty) \end{pmatrix} = \mathcal{M}\begin{pmatrix} a_x(u_T) \\ a_y(u_T) \\ a_z(u_T) \end{pmatrix}, \qquad (13)$$

where $\mathcal{M}$ is a 3×3 matrix having three eigenvalues. If an eigenvalue turns out to be vanishing at some momenta, the initial condition set with the corresponding eigenvector leads to the desired boundary conditions, $a_x(\infty) = a_y(\infty) = a_z(\infty) = 0$.

Figure 1 shows the smallest eigenvalue of $\mathcal{M}$ as a function of k_x and k_z (we can set $k_y = 0$ without loss of generality). We can get rid of u_T dependence by rescaling ρ, μ, B, and k_i. We find that $\rho = 3.72u_T^{5/2}$ is the critical value for $B = 0$ at which the smallest eigenvalue touches zero at $|\boldsymbol{k}| = 2.3u_T^{1/2}$ (which confirms Ref. [20]). When we increase B, the smallest eigenvalue is pushed up, as depicted by the upper surface in Fig. 1, and thus the critical density should get larger. This means that a larger B disfavors the spatially modulated phase. Though it is not visually clear from Fig. 1, the eigenvalue is slightly tilted in the presence of B, and the minimum of the eigenvalues is located on $k_x \neq 0$ and $k_z = 0$.

In terms of the chemical potential, the relation between μ_c and B is more complicated. As seen by the solid curve in Fig. 2, μ_c rather goes down with increasing B as long as

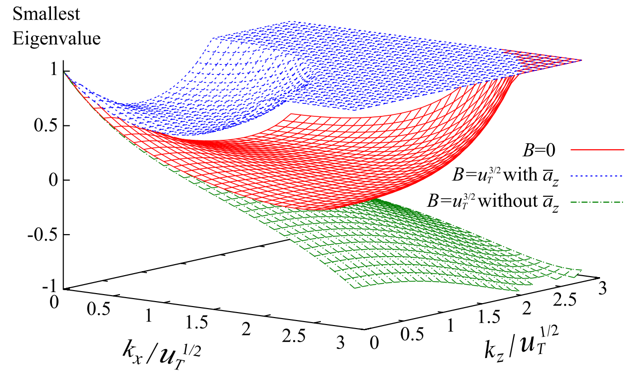

FIG. 1 (color online). Smallest eigenvalue of the matrix $\mathcal{M}$ as a function of k_x (perpendicular to B) and k_z (parallel to B) at $\rho = 3.72u_T^{5/2}$ at $B = 0$ (surface in the middle) and at $B = u_T^{3/2}$ with $\bar{a}_z$ (surface in the top) and without $\bar{a}_z$ (surface in the bottom).

the magnetic field is small enough, $B/u_T^{3/2} \lesssim 1$, even though the critical ρ monotonically grows up. This is simply because the phase space is enhanced by B; if B is raised up for a fixed μ, the corresponding density ρ becomes larger.

Discussion.—It could have been more intuitively understandable if B favored more modulation in view of the chiral magnetic spirals at $B \to \infty$. Here, in order to think of the effect of the topological current (2), let us drop off $\bar{a}_z(u)$ from the calculation. Of course, $\bar{a}_z(u) = 0$ is not a solution of the equation of motion, but this artificial manipulation in the present holographic treatment can mimic the common approximation to neglect $\boldsymbol{j}_A$ in most nonholographic calculations.

In this case, without $\bar{a}_z$ we find that the smallest eigenvalue is significantly pushed down by B, as seen in the bottom surface in Fig. 1. This indicates that the critical density is lowered by B, which makes a sharp contrast to

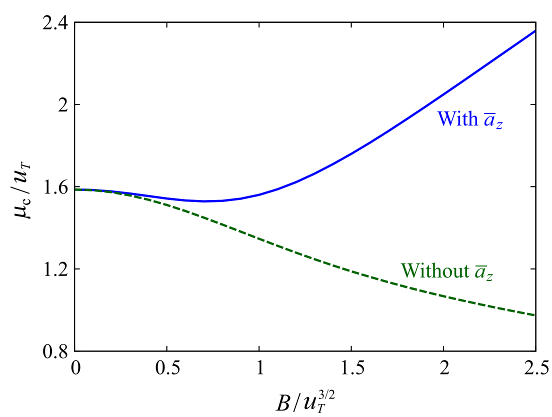

FIG. 2 (color online). Critical chemical potential μ_c as a function of B. The upper solid curve represents the result with $\bar{a}_z$ taken into account, and the lower dashed line represents the result without $\bar{a}_z$.

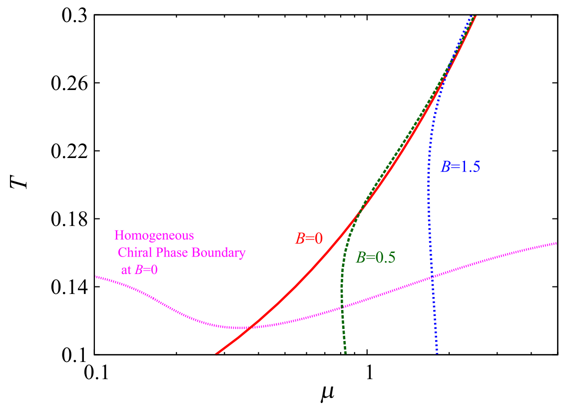

FIG. 3 (color online). Phase boundaries of the onset of the spatially modulated phase at $B = 0$ (solid curve), $B = 0.5$ (dashed curve), and $B = 1.5$ (dotted curve) not in the unit of u_T but in the AdS radius. For reference, the phase boundary for the homogeneous chiral transition [26] is also shown.

the case with $\bar{a}_z$ (and thus $\boldsymbol{j}_A$). Needless to say, the critical chemical potential μ_c also exhibits an opposite behavior to the previous case with $\bar{a}_z$, which is evident from the dashed curve in Fig. 2.

In the holographic approach, generally, it is hard to carve distinct physical effects out from the final results, and we did not spell out the axial-vector interaction $\sim(\bar{\psi}\gamma_5\gamma_\mu\boldsymbol{\tau}\psi)^2$. Nevertheless, our finding based on the comparison with and without $\bar{a}_z$ is suggestive enough to demonstrate the importance of the axial-vector interaction along the same direction as the Landau-Migdal interaction disfavoring the p-wave pion condensation. It is an intriguing future problem to implement the axial-vector interaction in conventional chiral models such as the (Polyakov-loop coupled) Nambu–Jona-Lasinio model and the quark-meson model to confirm our finding and elucidate more microscopic dynamics. In fact, in these chiral models, $\boldsymbol{j}_A$ should be treated as a mean-field variable and $\boldsymbol{j}_A$ is then "renormalized" [24]. Similar corrections on the topological current are reported also with explicit QED calculations [25].

Summary.—We calculated the critical density and the critical chemical potential μ_c for spatial modulation at finite B. We found that the spatial modulation was disfavored for a larger B, which became manifest on the phase diagram as summarized in Fig. 3. When $B = 0$, we could find $\mu_c \simeq 1.59u_T = 27.9T^2$ that drew a solid curve in Fig. 3 (as seen in Ref. [20]). This phase boundary was shifted toward larger μ with increasing B so that a stronger B caused shrinkage of the region with spatial inhomogeneity on the phase diagram. The effect of B appeared tamed at higher T, which could be explained from Eq. (5) in which B^2/u_T^3 became negligible for high T and thus large u_T. By comparing the results with and without the background $\bar{a}_z(u)$, we concluded that the disfavor of the spatially modulated phase at finite B was attributed to the topological currents and presumably the axial-vector interaction strengthened by $\boldsymbol{j}_A$.

We are now making progress to explore the whole structure of the holographic QCD phase diagram at finite T, μ, and B including the effect of spontaneous chiral-symmetry breaking and baryon density source that both make $x_4(u)$ take a nontrivial shape. This will be reported elsewhere.

We thank S. Nakamura, I. Shovkovy, and W. Weise for useful discussions. K. F. was supported by JSPS KAKENHI Grant No. 24740169.

[1] For reviews, see S. Muroya, A. Nakamura, C. Nonaka, and T. Takaishi, Prog. Theor. Phys. **110**, 615 (2003); K. Fukushima and T. Hatsuda, Rep. Prog. Phys. **74**, 014001 (2011).
[2] T. K. Herbst, J. M. Pawlowski, and B.-J. Schaefer, Phys. Rev. D **88**, 014007 (2013).
[3] M. Asakawa and K. Yazaki, Nucl. Phys. **A504**, 668 (1989); A. Barducci, R. Casalbuoni, S. De Curtis, R. Gatto, and G. Pettini, Phys. Lett. B **231**, 463 (1989); A. Barducci, R. Casalbuoni, G. Pettini, and R. Gatto, Phys. Rev. D **49**, 426 (1994).
[4] L. Kumar (STAR Collaboration), Nucl. Phys. **A904-905**, 256 (2013); J. T. Mitchell (PHENIX Collaboration), Nucl. Phys. **A904-905**, 903 (2013).
[5] M. Kitazawa, T. Koide, T. Kunihiro, and Y. Nemoto, Prog. Theor. Phys. **108**, 929 (2002); C. Sasaki, B. Friman, and K. Redlich, Phys. Rev. D **75**, 074013 (2007); K. Fukushima, Phys. Rev. D **78**, 114019 (2008).
[6] K. Fukushima, Phys. Rev. D **86**, 054002 (2012).
[7] G. A. Contrera, A. G. Grunfeld, and D. B. Blaschke, arXiv:1207.4890.
[8] D. V. Deryagin, D. Y. Grigoriev, and V. A. Rubakov, Int. J. Mod. Phys. A **07**, 659 (1992); E. Shuster and D. T. Son, Nucl. Phys. **B573**, 434 (2000); E. Nakano and T. Tatsumi, Phys. Rev. D **71**, 114006 (2005); D. Nickel, Phys. Rev. D **80**, 074025 (2009); T. Kojo, Y. Hidaka, L. McLerran, and R. D. Pisarski, Nucl. Phys. **A843**, 37 (2010).
[9] S. Carignano, D. Nickel, and M. Buballa, Phys. Rev. D **82**, 054009 (2010).
[10] For a comprehensive collection of reviews, see R. Tamagaki *et al.*, Prog. Theor. Phys. Suppl. **112**, 1 (1993)..
[11] T. Tatsumi, arXiv:nucl-th/0302009.
[12] T. Sakai and S. Sugimoto, Prog. Theor. Phys. **113**, 843 (2005).
[13] F. Preis, A. Rebhan, and A. Schmitt, J. High Energy Phys. 03 (2011) 033.
[14] F. Preis, A. Rebhan, and A. Schmitt, Lect. Notes Phys. **871**, 51 (2013).
[15] V. P. Gusynin, V. A. Miransky, and I. A. Shovkovy, Phys. Rev. Lett. **73**, 3499 (1994); Phys. Rev. D **52**, 4718 (1995).
[16] For recent reviews, see R. Gatto and M. Ruggieri, Lect. Notes Phys. **871**, 87 (2013); E. S. Fraga, Lect. Notes Phys. **871**, 121 (2013).
[17] G. Basar, G. V. Dunne, and D. E. Kharzeev, Phys. Rev. Lett. **104**, 232301 (2010).

[18] E. J. Ferrer, V. de la Incera, and A. Sanchez, Acta Phys. Pol. B **5**, 679 (2012).
[19] M. A. Metlitski and A. R. Zhitnitsky, Phys. Rev. D **72**, 045011 (2005); K. Fukushima, D. E. Kharzeev, and H. J. Warringa, Phys. Rev. D **78**, 074033 (2008); A. Vilenkin, Phys. Rev. D **22**, 3080 (1980); M. Giovannini and M. E. Shaposhnikov, Phys. Rev. D **57**, 2186 (1998).
[20] H. Ooguri and C.-S. Park, Phys. Rev. Lett. **106**, 061601 (2011); W.-y. Chuang, S.-H. Dai, S. Kawamoto, F.-L. Lin, and C.-P. Yeh, Phys. Rev. D **83**, 106003 (2011).
[21] A. Ballon-Bayona, K. Peeters, and M. Zamaklar, J. High Energy Phys. 11 (2012) 164.
[22] E. Witten, Adv. Theor. Math. Phys. **2**, 505 (1998).
[23] H.-U. Yee, J. High Energy Phys. 11 (2009) 085; A. Rebhan, A. Schmitt, and S. A. Stricker, J. High Energy Phys. 01 (2010) 026.
[24] K. Fukushima and M. Ruggieri, Phys. Rev. D **82**, 054001 (2010).
[25] E. V. Gorbar, V. A. Miransky, I. A. Shovkovy, and X. Wang, Phys. Rev. D **88**, 025025 (2013).
[26] O. Bergman, G. Lifschytz, and M. Lippert, J. High Energy Phys. 11 (2007) 056.